Anharmonic vibrational properties of CH2F2 : A comparison of theory and experiment

R. D. Amos, N. C. Handy, W. H. Green, D. Jayatilaka, A. Willetts, and P. Palmieri

Citation: The Journal of Chemical Physics **95**, 8323 (1991); doi: 10.1063/1.461259
View online: http://dx.doi.org/10.1063/1.461259
View Table of Contents: http://scitation.aip.org/content/aip/journal/jcp/95/11?ver=pdfcov
Published by the AIP Publishing

Anharmonic vibrational properties of CH_2F_2: A comparison of theory and experiment

R. D. Amos, N. C. Handy, W. H. Green, D. Jayatilaka, and A. Willetts
University Chemical Laboratory, Cambridge CB2 1EW, United Kingdom

P. Palmieri
Dipartimento di Chimica Fisica ed Inorganica, Viale Risorgimento 4, 40136 Bologna, Italy

(Received 18 March 1991; accepted 12 August 1991)

Ab initio theoretical chemistry is used to provide a complete understanding of the infrared spectroscopy of CH_2F_2. Second-order Møller–Plesset perturbation theory (MP2) with a 631G extended basis set is used to provide a quartic expansion of the potential energy surface and a cubic expansion of the dipole surface. Standard perturbation theory is then used to determine effective vibrational and rotational Hamiltonians for fundamentals, selected overtones, and combination bands. Effects of Fermi resonance, Darling–Dennison resonance, and Coriolis resonance are included by matrix diagonalization. Empirical (x,K) relations are used to demonstrate that the anharmonic constants for C–H are in good agreement with those determined from CH_2Cl_2. The local mode nature of the CH overtones is demonstrated. Important resonances are found to be $(\nu_3,2\nu_4)$, $(\nu_8,\nu_4+\nu_9)$, and $(\nu_1,2\nu_2,2\nu_8,\nu_4+\nu_8+\nu_9, 2\nu_4+2\nu_9,\nu_3+2\nu_9)$. Rotational constants, quartic and sextic centrifugal distortion constants, vibration rotation interaction constants, and Coriolis constants are all in good agreement with the mass of experimental data. The signs of the dipole moment derivatives are in agreement with those deduced from experiment. The separate contributions to the infrared intensities from electrical, mechanical, and mixed anharmonicity are examined for fundamentals and overtones, but by far the most important effect arises from corrections due to resonant Fermi and Darling–Dennison interactions. In this way, the $2\nu_8$, ν_1 and ν_6 experimental bands and their intensities are explained by assigning ν_1 and ν_6 as $(\nu_1,\nu_4+\nu_8+\nu_9)$ and $(\nu_6,2\nu_2)$ doublets, respectively. This paper therefore demonstrates that state of the art quantum chemistry can provide a complete interpretation of such spectroscopic data.

I. INTRODUCTION

A large amount of spectroscopic infrared and microwave data has now been collected for CH_2F_2. Harmonic frequencies and force field have been determined by Suzuki and Shimanouchi[1]; the ground state microwave spectrum, first recorded by Koutcher[2], has been reported recently by Martinache *et al.*[3] The microwave spectra of several excited vibrational states have been also reported by Hirota[4] with a detailed analysis of the cubic force field.[5] More recently, interest on this molecule has been focused on the far infrared,[6] mainly due to its high lasing efficiency in this spectral region.[7–9] At the opposite side of the infrared, the vibrational overtone spectrum has been measured up to the sixth overtone of the C–H stretching vibration[10] and interpreted using "a local mode" description.[11]

The infrared intensities of this molecule have been discussed in detail by several authors.[12–16] The rotationless transition dipole moment of the ν_9 fundamental, which plays an important role in determining the lasing efficiency of the molecule in the far infrared, has been determined by sub-Doppler molecular beam CO_2 laser Stark spectroscopy.[17]

Quantum mechanical computations can in principle provide a compact description of all these spectroscopic properties through the accurate representation of the intramolecular force and dipole fields and, in fact, they have played an important role in the interpretation and determination of the spectroscopic properties of this molecule. Using *ab initio* self-consistent field (SCF) methods, harmonic[18] and more recently the cubic[19] molecular force fields have been determined and are able to reproduce accurately harmonic frequencies, centrifugal distortion, and vibration–rotation interaction constants. The determination of the atomic polar tensors from the integrated infrared molar absorption coefficients often relies on the comparison beween empirical and theoretical values of the tensor components.[12–16]

It is now recognized that the inclusion of electron correlation effects is important for the accurate prediction of spectroscopic properties.[20–23] Fox and Schlegel[24] have used Møller–Plesset second-order perturbation theory (MP2), which is the simplest of the correlated method for electron structure computations and obtained accurate theoretical values of the harmonic frequencies and double-harmonic intensities of this molecule.

We have extended this study to a comprehensive analysis of the vibrational properties of CH_2F_2 using analytical procedures[22] and programs[25] which provide first and second derivatives of MP2 energies. This has allowed the inclusion of anharmonic effects, which have been neglected in most of the previous theoretical studies and are important due to the near degeneracy of several fundamental molecular

 0021-9606/91/238323-14$03.00

vibrations. In particular, we have used a quartic representation for the force field and cubic representations for the dipole fields.

Despite recent advances on variational treatments of anharmonicity,[26–29] second-order perturbation theory, which provides the exact value of the x anharmonic constant of a Morse oscillator,[30] and closed expressions for most of the spectroscopic parameters required for the analysis of the experimental frequencies and intensities[31–36] appears more generally suited for polyatomic molecules of moderate complexity. Therefore, we base our study on this classical perturbation approach to anharmonicity effects in polyatomic molecules[32–36] introducing resonance effects by matrix diagonalizations. The computational scheme and programs have been described recently.[37,38]

II. THE ANHARMONIC CORRECTIONS TO FREQUENCIES AND INTENSITIES

We refer to the literature for all details[31–36] but give a brief outline to make the presentation self-contained and list the main equations and symbols used for the present study.

A. The effective vibrational Hamiltonian

Here we explain the analysis we use for the treatment of resonance effects in our vibrational studies. We start by expressing the vibrational Hamiltonian $\mathbf{H}_{\rm vib}$ using reduced normal coordinates q_r,[33–35] harmonic frequencies ω_r, and wave number units as a sum of the zero-order harmonic term $\mathbf{H}^0_{\rm vib}$, first-order term $\mathbf{H}^1_{\rm vib}$ with the cubic components of the potential, and a second-order term $\mathbf{H}^2_{\rm vib}$ including all quartic components of the potential and the kinetic energy corrections arising from the vibrational angular momentum j_α:

$$\begin{aligned}\mathbf{H}_{\rm vib} &= \mathbf{H}^0_{\rm vib} + \mathbf{H}^1_{\rm vib} + \mathbf{H}^2_{\rm vib}\\ &= \frac{1}{2}\sum_r \omega_r(p_r^2+q_r^2) + \frac{1}{6}\sum_{rst}\phi_{rst}q_rq_sq_t\\ &\quad + \frac{1}{24}\sum_{rstu}\phi_{rstu}q_rq_sq_tq_u + \sum_\alpha B^e_\alpha j_\alpha^2. \end{aligned} \tag{1}$$

ϕ_{rst},ϕ_{rstu} are the cubic and quartic force constants, α identifies a rotational axis, and B^e_α the corresponding equilibrium rotational constant.

For a given set of vibrational states, we identify all terms of Eq. (1), i.e., $\mathbf{H}^{1*}_{\rm vib}$, $\mathbf{H}^{2*}_{\rm vib}$, which generate resonant or nearly resonant interactions between the corresponding solutions of the harmonic problem $\{|\mathbf{v}^0_i\rangle,|\mathbf{v}^0_j\rangle\}$. From these solutions, the vibrational wave functions $\{|\mathbf{v}_i\rangle,|\mathbf{v}_j\rangle\}$ are obtained by second-order perturbation theory

$$|\mathbf{v}_i\rangle = |\mathbf{v}^0_i\rangle + |\mathbf{v}^1_i\rangle + |\mathbf{v}^2_i\rangle \tag{2}$$

using all nonresonant energy terms in Eq. (1) followed by a variational treatment of the relevant $\mathbf{H}^{1*}_{\rm vib}$, $\mathbf{H}^{2*}_{\rm vib}$ resonant interactions. Here $|\mathbf{v}^0_i\rangle$ stands for the vector $|...,v_r,...,v_s\rangle$, or for brevity $|v_r,v_s\rangle$, with all required vibrational quantum numbers required to specify the zero-order harmonic solution.

This leads to an effective vibrational Hamiltonian matrix for the nearly degenerate set of $\{|\mathbf{v}_i\rangle,|\mathbf{v}_j\rangle\}$ states, which can be written in the form

$$\begin{aligned}\langle\mathbf{v}_i|\mathbf{H}^{\rm eff}_{\rm vib}|\mathbf{v}_j\rangle &= \langle\mathbf{v}^0_i|\mathbf{H}^2_{\rm vib}|\mathbf{v}^0_j\rangle + \langle\mathbf{v}^1_i|\mathbf{H}^1_{\rm vib}|\mathbf{v}^0_j\rangle\\ &\quad + \langle\mathbf{v}^0_i|\mathbf{H}^1_{\rm vib}|\mathbf{v}^1_j\rangle. \end{aligned} \tag{3}$$

The diagonal elements of the effective Hamiltonian matrix are represented in the standard form

$$\begin{aligned}\langle\mathbf{v}_i|\mathbf{H}^{\rm eff}_{\rm vib}|\mathbf{v}_i\rangle &= \sum_r \omega_r\left(v_r+\frac{1}{2}\right) + \sum_{r\geq s} x_{rs}\left(v_r+\frac{1}{2}\right)\\ &\quad\times\left(v_s+\frac{1}{2}\right). \end{aligned} \tag{4}$$

By comparing Eqs. (3) and (4) as in the usual perturbation theory, the expressions of the anharmonic constants x_{rr},x_{rs} are derived

$$\begin{aligned}x_{rr} &= \frac{1}{16}\phi_{rrrr} - \sum_{t\{\omega_t\neq 2\omega_r\}}\Omega_{rt}(\omega_r,\omega_t)\phi^2_{rrt}\\ &\quad - \sum_{t\{\omega_t\simeq 2\omega_r\}}\Omega^*_{rt}(\omega_r,\omega_t)\phi^2_{rrt}, \end{aligned} \tag{5a}$$

$$\begin{aligned}x_{rs} &= \frac{1}{4}\phi_{rrss} - \sum_t\frac{\phi_{rrt}\phi_{sst}}{4\omega_t} - \sum_{t\{\omega_r+\omega_s\neq\omega_t\}}\Omega_{rst}(\omega_r,\omega_s,\omega_t)\\ &\quad\times\phi^2_{rst} + \sum_\alpha B^e_\alpha(\zeta^\alpha_{rs})^2\left(\frac{\omega_r}{\omega_s}+\frac{\omega_s}{\omega_r}\right)\\ &\quad - \sum_{t\{\omega_r+\omega_s\simeq\omega_t\}}\Omega^*_{rst}(\omega_r,\omega_s,\omega_t)\phi^2_{rst}. \end{aligned} \tag{5b}$$

In Eqs. (5a) and (5b), the weighting factors of the resonant Ω^* and nonresonant Ω contributions are, respectively,

$$\Omega_{rt}(\omega_r,\omega_t) = \frac{(8\omega_r^2-3\omega_t^2)}{16\omega_t(4\omega_r^2-\omega_t^2)}, \tag{6a}$$

$$\Omega^*_{rt}(\omega_r,\omega_t) = \frac{1}{8}\left[\frac{1}{\omega_t}+\frac{1}{4(2\omega_r+\omega_t)}\right], \tag{6b}$$

$$\Omega_{rst}(\omega_r,\omega_s,\omega_t) = \frac{\omega_t(\omega_r^2+\omega_s^2-\omega_t^2)}{2(\omega_r+\omega_s+\omega_t)(-\omega_r+\omega_s+\omega_t)(\omega_r-\omega_s+\omega_t)(\omega_r+\omega_s-\omega_t)}, \tag{6c}$$

$$\Omega^*_{rst}(\omega_r,\omega_s,\omega_t) = \frac{1}{8}\left[\frac{1}{(\omega_r+\omega_s+\omega_t)}+\frac{1}{(\omega_r-\omega_s+\omega_t)}+\frac{1}{(-\omega_r+\omega_s+\omega_t)}\right]. \tag{6d}$$

We shall restrict our analysis of resonant effects to off-diagonal matrix elements of Fermi [Eqs. (7a) and (7b)][39] and Darling–Dennison [Eq. (7c)][40] types

$$\langle v_r+1,v_s+1,v_t|\mathbf{H}^{\rm eff}_{\rm vib}|v_r v_s v_t+1\rangle = \phi_{rst}\sqrt{\frac{(v_r+1)(v_s+1)(v_t+1)}{8}}, \tag{7a}$$

$$\langle v_r+2,v_t|\mathbf{H}^{\rm eff}_{\rm vib}|v_r,v_t+1\rangle = \frac{\phi_{rrt}}{4}\sqrt{\frac{(v_r+2)(v_r+1)(v_t+1)}{2}}, \tag{7b}$$

$$\langle v_r+2,v_t|\mathbf{H}^{\rm eff}_{\rm vib}|v_r,v_t+2\rangle = \frac{K_{rrtt}}{4}\sqrt{(v_r+1)(v_r+2)(v_t+1)(v_t+2)}. \tag{7c}$$

The general expression of the K_{rrtt} effective quartic force constants is again obtained by comparing Eqs. (3) and (7c)

$$K_{rrss} = \frac{\phi_{rrss}}{4} - 4\sum_\alpha B^e_\alpha(\zeta^\alpha_{rs})^2 + \frac{1}{6(\omega_r+\omega_s)}(\phi_{rrr}\phi_{rss}+\phi_{sss}\phi_{srr}) + \frac{1}{4}\sum_t \frac{\omega_t}{[(\omega_r+\omega_s)^2-\omega_t^2]}\phi_{rrt}\phi_{tss} - \frac{\phi^2_{rss}}{2\omega_s} - \frac{\phi^2_{srr}}{2\omega_r} - \sum_t \frac{\phi^2_{rst}}{2\omega_t}, \tag{8}$$

where ζ^α_{rs} is a Coriolis coupling constant.

B. The effective rotational Hamiltonian

The vibrotational Hamiltonian $\mathbf{H}_{\rm vibrot}$ is obtained by adding to Eq. (1) the rotational energy terms

$$\mathbf{H}_{\rm vibrot} = \mathbf{H}_{\rm vib} + \sum_\alpha B^e_\alpha J^2_\alpha + \sum_{\alpha,\beta}\sum_r B^{\alpha\beta}_r q_r J_\alpha J_\beta + \frac{1}{2}\sum_{\alpha,\beta}\sum_{rs} B^{\alpha\beta}_{rs} q_r q_s J_\alpha J_\beta - 2\sum_\alpha B_\alpha J_\alpha j_\alpha. \tag{9}$$

This includes the centrifugal distortion energy terms and the Coriolis coupling between vibrational j_α and rotational J_α angular momenta; $B^e_\alpha, B^{\alpha\beta}_r, B^{\alpha\beta}_{rs}$ are the rotational constants and their derivatives with respect to normal coordinates. Alternatively, the rotational energy terms are expressed using the inertial principal moments $I^e_{\alpha\alpha}$ and the inertial derivatives $a^{\alpha\beta}_r, a^{\alpha\beta}_{rs}$.

The procedure summarized by Eqs. (1) and (3) can now be repeated to obtain an effective rotational Hamiltonian matrix inclusive of all quartic centrifugal distortion energy terms, from which vibrotational eigenfunctions $|\mathbf{v}_i J\rangle$ and energies are obtained. The procedure to account for sextic centrifugal distortions is more elaborate requiring the extension of the perturbation treatment to fourth order with respect to selected components of the Hamiltonian (9).[35]

We shall refer to the effective rotational Hamiltonian in its reduced A form in the Ir representation

$$\mathbf{H}^{vJ}_{\rm eff} = \sum_\alpha B^v_\alpha J^2_\alpha - \Delta_J \mathbf{J}^4 - \Delta_{Jk}\mathbf{J}^2\mathbf{J}^2_z - \Delta_k \mathbf{J}^4_z - \frac{1}{2}[(\delta_J\mathbf{J}^2+\delta_k\mathbf{J}^2_z),(\mathbf{J}^2_+ + \mathbf{J}^2_-)]_+ + \Phi_J\mathbf{J}^6 + \Phi_{Jk}\mathbf{J}^4\mathbf{J}^2_z + \Phi_{kJ}\mathbf{J}^2\mathbf{J}^4_z + \Phi_k\mathbf{J}^6_z + \frac{1}{2}[(\phi_J\mathbf{J}^4+\phi_{Jk}\mathbf{J}^2\mathbf{J}^2_z+\phi_k\mathbf{J}^4_z),(\mathbf{J}^2_+ + \mathbf{J}^2_-)]_+, \tag{10}$$

the effective rotational constant B^v_α:

$$B^v_\beta = B^e_\beta - \sum_r \alpha^\beta_r\left(v_r+\frac{1}{2}\right) \tag{11}$$

being defined through the vibrotational anharmonic constant α^β_r:

$$-\alpha^\beta_r = \frac{2(B^e_\beta)^2}{\omega_r}\left[\sum_\alpha \frac{3}{4}\frac{(a^{\alpha\beta}_r)^2}{I^e_{\alpha\alpha}} + \sum_{s\{\omega_r\neq\omega_s\}}\frac{(3\omega_r^2+\omega_s^2)}{(\omega_r^2-\omega_s^2)}\times(\zeta^\beta_{rs})^2 - \sum_{s\{\omega_r\simeq\omega_s\}}\frac{(\omega_r-\omega_s)^2}{2\omega_r\omega_s(\omega_r+\omega_s)}(\zeta^\beta_{rs})^2 + \pi\sqrt{\frac{c}{h}}\sum_{s\{\omega_s\neq 2\omega_r\}}\frac{\phi_{rrs}a^{\beta\beta}_s\omega_r}{\omega_s\sqrt{\omega_s}}\right]. \tag{12}$$

The second and the third summations in Eq. (12) are restricted to nonresonant and to resonant Coriolis interacting modes, respectively. The latter, in addition to the diagonal blocks $\langle Jk|\mathbf{H}^{vJ}_{\rm eff}|Jk\rangle$ generate off-diagonal blocks of matrix elements, which are cast in the form

$$\langle \mathbf{v}J|\mathbf{H}_{\rm vibrot}|\mathbf{v}'J\rangle = i\sum_\beta \xi^\beta_{\mathbf{v}'\mathbf{v}}\langle Jk|\mathbf{J}_\beta|Jk'\rangle, \tag{13}$$

where $|Jk\rangle$ are symmetric top wave functions. The resonant Fermi contributions, being excluded from the last summation in Eq. (12), are taken into account by weighting the $B^{\rm v}_\beta$ values over the resonant states using the vibrational wave functions resulting from the diagonalization of the corresponding $\mathbf{H}^{\rm eff}_{\rm vib}$ matrix (3).

The detailed expressions of all remaining centrifugal distortion constants in terms of harmonic and cubic force constants, rotational constants, and derivatives are found in Refs. 34 and 35.

C. Harmonic and anharmonic contributions to vibrational band intensities

In analogy with Eq. (1), the dipole moment expansion about the equilibrium geometry

$$\mu^\alpha = \mu^0_\alpha + \mu^1_\alpha + \mu^2_\alpha = (\mu^\alpha)^e + \sum_r \mu^\alpha_r q_r + \frac{1}{2}\sum_{rs}\mu^\alpha_{rs}q_r q_s + \frac{1}{6}\sum_{rst}\mu^\alpha_{rst}q_r q_s q_t \tag{14}$$

is partitioned into a zero-order linear, first-order quadratic, and second-order cubic components.

From the vibrational wave functions (2), the following contributions to the transition dipole moment are obtained:

$$\langle v_i^0|\mu_\alpha^0|v_j^0\rangle, \tag{15a}$$
$$\langle v_i^0|\mu_\alpha^1|v_j^0\rangle, \tag{15b}$$
$$\langle v_i^0|\mu_\alpha^0|v_j^1\rangle + \langle v_i^1|\mu_\alpha^0|v_j^0\rangle, \tag{15c}$$
$$\langle v_i^0|\mu_\alpha^2|v_j^0\rangle, \tag{15d}$$
$$\langle v_i^0|\mu_\alpha^1|v_j^1\rangle + \langle v_i^1|\mu_\alpha^1|v_j^0\rangle, \tag{15e}$$
$$\langle v_i^0|\mu_\alpha^0|v_j^2\rangle + \langle v_i^2|\mu_\alpha^0|v_j^0\rangle, \tag{15f}$$
$$\langle v_i^1|\mu_\alpha^0|v_j^1\rangle. \tag{15g}$$

For fundamentals, the first-order contributions (15b) and (15c) vanish identically and one is left with the second-order electric [Eq. (15d)], mixed mechanical–electric [Eq. (15e)], quartic [Eq. (15f)], and cubic [Eq. (15g)] anharmonic corrections to the harmonic transition moment (15a). The two components (15a) and (15d) are polarized equally; all remaining contributions have mixed polarizations and contribute to the mixed character of the band. For overtones and combination bands, only the first-order electric [Eq. (15b)] and mechanical [Eq. (15b)] corrections survive. For resonant vibrational levels, the final transition moments are obtained by linear combinations of the terms above.

III. THE METHOD OF COMPUTATION

The equilibrium geometry, the harmonic force field, the normal coordinates, and the electric dipole derivatives have been evaluated analytically by the MP2 method using the Cambridge analytic derivatives package (CADPAC)[25] suite of programs and the 631 G extended[41,42] basis of contracted Gaussian functions, inclusive of polarization functions on heavy atoms and hydrogens.

We differentiate the potential function in the Hamiltonian (1) to derive the general expressions of the harmonic force constants $\phi_{rs}(q_t,q_u)$ for arbitrary molecular geometries as specified by the values of the reduced normal coordinates q_t,q_u differing from the equilibrium values

$$\phi_{rs}(q_t,q_u) = \omega_r\delta_{rt}\delta_{st} + \omega_s\delta_{ru}\delta_{su} + \phi_{rst}q_t + \phi_{rsu}q_u + \phi_{rstu}q_tq_u + \tfrac{1}{2}\phi_{rstt}q_t^2 + \tfrac{1}{2}\phi_{rsuu}q_u^2. \tag{16}$$

By finite differences of the harmonic force constants evaluated analytically at various geometries, the cubic and quartic force fields over reduced normal coordinates may therefore be obtained.

$2(3N-6)$ force field evaluations are generally required to determine all cubic ϕ_{rst} [Eq. (17a)] and diagonal ϕ_{rsrs} and semidiagonal ϕ_{rrst} [Eq. (17b)] quartic force constants

$$\phi_{rst} = \frac{\phi_{st}(q_r) - \phi_{st}(-q_r)}{2q_r}, \tag{17a}$$
$$\phi_{rrst} = \frac{\phi_{st}(q_r) - 2\omega_r\delta_{st} + \phi_{st}(-q_r)}{q_r^2}. \tag{17b}$$

One of the disadvantages of Eqs. (17a) and (17b) is that, by taking the displacements along the reduced normal coordinates $\{q_r\}$, the molecular symmetry can only be partially exploited; moreover, whenever required, one must determine by separate computations the cubic and quartic force fields of different molecular isotopes. On the other hand, by Eqs. (17a) and (17b), we evaluate all constants needed for the perturbative treatment described in the previous section.[43]

Many more harmonic force fields would be needed $(3N-7)\times(3N-6)$ to determine all remaining quartic force constants

$$\phi_{rstu} = \frac{\phi_{rs}(q_t,q_u) + \phi_{rs}(-q_t,-q_u) - \phi_{rstt}q_t^2 - \phi_{rsuu}q_u^2}{2q_tq_u}, \tag{18}$$

this being the main computational advantage of the perturbation approach compared to a full variational treatment of vibration–rotation levels in polyatomic molecules based on normal or other internal coordinates.

Similarly, from the MP2 dipole first derivatives $\mu_r^\alpha(q_s)$ evaluated at different geometries, the linear, quadratic, and cubic coefficients of the dipole expansion are obtained:

$$\mu_r^\alpha(q_s) = \mu_r^\alpha + \mu_{rs}^\alpha q_s + \tfrac{1}{2}\mu_{rss}^\alpha q_s^2 \tag{19}$$

giving

$$\mu_{rs}^\alpha = \frac{\mu_r^\alpha(q_s) - \mu_r^\alpha(-q_s)}{2q_s}, \tag{20a}$$
$$\mu_{rss}^\alpha = \frac{\mu_r^\alpha(q_s) - 2\mu_r^\alpha + \mu_r^\alpha(-q_s)}{q_s^2}. \tag{20b}$$

Based on a maximum energy difference between the resonant states (200 cm^{-1}) and the minimum absolute value of the interaction constants (0.25 for Coriolis couplings and 10 cm^{-1} for the cubic force constants), thresholds for the resonant terms in Eqs. (5a) and (5b) are set. The effective vibrational [Eq. (3)] and rotational [Eq. (10)] Hamiltonians are obtained, the matrix elements (7) and (10) and all contributions (15) to the vibrational band intensities being evaluated from Eqs. (17) and (20). All spectroscopic constants in the effective vibrational and vibrotational Hamiltonians have been evaluated independently at the two laboratories by using two different computer programs[19,37]; the second of the two programs (SPECTRO[37]) was used to evaluate infrared intensities.

IV. RESULTS AND DISCUSSION

The computed equilibrium molecular geometry is reported in Table I and shows good agreement with previous

TABLE I. (a) Experimental r_s; (b) r_e molecular structures (Ref. 5); and (c) computed MP2 equilibrium geometry for CH_2F_2. Bond distances are in Angstroms and angles in degrees.

	(a)	(b)	(c)
C–H	1.0934	1.084	1.0907
C–F	1.3574	1.3508	1.3662
H–C–H	113.7	112.8	113.7
F–C–F	108.3	108.5	108.6
H–C–F	108.7	108.9	108.6

theoretical results by the MP2 method.[24] Compared to the structure derived experimentally by Hirota,[5] the discrepancies are 0.0067 Å for the C–H and 0.0154 Å for the C–F bond lengths.

A. Anharmonic force field and frequencies

The MP2 harmonic frequencies listed in Table II lie very close to the MP2 limit estimated from a series of computations with orbital bases of increasing accuracy.[24] The remaining discrepancy from the empirical values[18] may be due either to the correlation energy terms not accounted for by MP2 or to the method used[43] to derive the harmonic from the experimental frequencies. The results in this table are a further demonstration that MP2 is a very good model for single bonded systems.

The MP2 anharmonic cubic force constants are given in Table III; their accuracy can be assessed easily by comparison with the cubic force field of Ref. 19, where the *ab initio* SCF force constants have been scaled to reproduce the vibration–rotation interaction constants of CH_2F_2 and CD_2F_2. After converting the MP2 cubic force field from reduced normal ϕ_{rst} to curvilinear symmetry coordinates f_{rst} by standard tensor transformation,[45] the comparison is satisfactory, providing support to the scaling procedure and confirming the cubic force field of Ref. 19. The only serious discrepancy is f_{222} which we have evaluated -28.1 (cm^{-1}) to be compared with the scaled *ab initio* value of -43.5. However, it is particularly pleasing how well many of the smaller constants in columns (b) and (c) agree.

No direct experimental information is available on the quartic force field. Indirect information on these quantities come from the frequencies and anharmonic constants to be discussed below; the diagonal components computed for reduced normal coordinates by Eqs. (17) are listed in Table IV.

From the force field in Tables II–IV using Eqs. (5) and (8), we evaluate the anharmonic constants x_{rs},K_{rrss} in Table V.

Due to the empirical x, K relationships between symmetric and asymmetric stretch vibrations[30]

$$x_{11} = x_{66} = \frac{1}{4}x_{16} = \frac{1}{4}K_{1166} = \frac{x_m}{2},$$

$$\omega_m = \frac{\omega_1 + \omega_6}{2},$$

$$\lambda = \frac{\omega_1 - \omega_6}{2},$$

the x_{rs},K_{rrss} constants are related to the (C–H)x_m,ω_m intrabond and to the (C–H)λ interbond parameters; therefore, the anharmonic constants for the CH stretching modes are to a large extent transferable from the related molecule CH_2Cl_2 for which a detailed analysis of the CH overtones and combination bands is available.[47] For the latter molecule, the CH anharmonic constants have been estimated[47]

$$x_{11} = -29.7,$$
$$x_{66} = -32.4,$$
$$x_{16} = -119.0,$$
$$K_{1166} = -119.0$$

and these compare well with the corresponding values in Table V, implying a value of the anharmonicity constant of the C–H bond in CH_2F_2 $x_m = -61$ cm^{-1} in good agreement with the results on methane.[30]

We next identify important resonant interactions leading to the following effective vibrational Hamiltonians:

$$\begin{matrix} \omega_3 \\ 2\omega_4 \end{matrix}\begin{pmatrix} 1087.10 & -2.64 \\ -2.64 & 1033.80 \end{pmatrix} \tag{21}$$

for the ν_3 fundamental and the $2\nu_4$ overtone;

$$\begin{matrix} \omega_8 \\ \omega_4 + \omega_9 \end{matrix}\begin{pmatrix} 1447.40 & 14.13 \\ 14.13 & 1569.68 \end{pmatrix} \tag{22}$$

for ν_8 and for the $\nu_4 + \nu_9$ combination. The effective Hamiltonian matrix for the CH stretching modes ν_1,ν_6 is more complex due to the strong Fermi resonances $\nu_1 - 2\nu_2$, $\nu_1 - 2\nu_8$, and the $2\nu_2 - 2\nu_8$ Darling–Dennison interaction. The full polyad takes the following form:

$$\begin{matrix} \omega_1 \\ 2\omega_2 \\ 2\omega_8 \\ \omega_4 + \omega_8 + \omega_9 \\ 2\omega_4 + 2\omega_9 \\ \omega_3 + 2\omega_9 \end{matrix}\begin{pmatrix} 2980.6 & 40.0 & 65.5 & 0.0 & 0.0 & 0.0 \\ 40.0 & 3034.0 & -28.2 & 0.0 & 0.0 & 0.0 \\ 65.5 & -28.2 & 2894.8 & 20.0 & 0.0 & 0.0 \\ 0.0 & 0.0 & 20.0 & 3007.6 & 28.3 & 0.0 \\ 0.0 & 0.0 & 0.0 & 28.3 & 3117.4 & -2.6 \\ 0.0 & 0.0 & 0.0 & 0.0 & -2.6 & 3172.1 \end{pmatrix}. \tag{23}$$

From the polyads $\{\omega_2 + \omega_4 + \omega_9, \omega_2 + \omega_8\}$, $\{\omega_3 + \omega_4, 3\omega_4\}$, $\{\omega_3 + \omega_9, 2\omega_4 + \omega_9, \omega_4 + \omega_8\}$, $\{\omega_3 + \omega_7, 2\omega_4 + \omega_7\}$, $\{\omega_8 + \omega_9, \omega_4 + 2\omega_9\}$, and $\{\omega_3 + \omega_6, 2\omega_4 + \omega_6\}$, we derive additional overtones and combination frequencies for which experimental information is available.[1,4,16] Our results do not indicate important Fermi resonances for all remaining fundamentals, leading to the list of vibrational frequencies in Table VI. In line with previous experience with these methods,[20] there is on the whole very good agreement between theory and experiment, the greatest discrepancy as usual arising for the CH modes.

The structure of the infrared absorption system in the ν_1,ν_6 region is rather complex.[48–50] On the low frequency side, three bands have been identified—a *b*-type band at

TABLE II. The MP2 harmonic frequencies (cm^{-1}) of CH_2F_2: (a) present work; (b) the MP2 basis set limit from Ref. 24; (c) estimated from experimental frequencies (Ref. 18).

Symmetry		Mode	(a)	(b)	(c)
ω_1	A_1	CH_2 symmetric stretch	3133	3139	3071
ω_2	A_1	CH_2 scissor	1557	1550	1539
ω_3	A_1	CF_2 symmetric stretch	1109	1136	1124
ω_4	A_1	CF_2 bend	523	535	539
ω_5	A_2	CH_2 twist	1298	1292	1289
ω_6	B_1	CH_2 asymmetric stretch	3222	3216	3140
ω_7	B_1	CH_2 rock	1199	1197	1202
ω_8	B_2	CH_2 wag	1484	1474	1464
ω_9	B_2	CF_2 asymmetric stretch	1086	1120	1101

2838 cm^{-1} of moderate intensity and two nearly overlapping bands at 2948 cm^{-1} which have been assigned in the order to $2\nu_8, \nu_1, \nu_2 + \nu_8$, with ν_6 to higher frequency at 3014 cm^{-1}. As shown by Eq. (23), the strong Fermi resonance between ν_1 and $2\nu_8$ has been estimated at 65 cm^{-1} compared to a previous estimate of 52 cm^{-1};[51] we predict an additional $2\nu_8, \nu_4 + \nu_8 + \nu_9$ Fermi interaction of 20 cm^{-1} and the $2\nu_8, 2\nu_2$ Darling–Dennison coupling of 28 cm^{-1}.

The dimension of the effective Hamiltonian matrices increases rapidly with the vibrational energy. It becomes 21, 2, 6, and 10, respectively, for the vibrational frequencies of the four symmetry blocks in the region of the C–H stretching lowest overtone, leading to the $2\nu_1$, $\nu_1 + \nu_6$, and $2\nu_6$ frequencies in Table VI.

A simplified description is obtained by neglecting all interactions between C–H and the remaining normal modes. With this simplification, the polyad for the next higher C–H overtone becomes

TABLE III. The MP2 cubic force field (cm^{-1}) of CH_2F_2: (a) reduced normal coordinates ϕ_{rst}; (b) curvilinear internal coordinates f_{rst} (Ref. 46); (c) scaled *ab initio* cubic force field in curvilinear internal coordinates from Ref. 19.

ϕ_{rst}	(a)	(b)	(c)	ϕ_{rst}	(a)	(b)	(c)
ϕ_{111}	−1347.834	−22.575	−22.889	ϕ_{277}	−76.668	−1.398	−1.002
ϕ_{112}	11.221	0.334	0.380	ϕ_{288}	28.508	−23.773	−24.781
ϕ_{113}	21.105	−0.158	−0.184	ϕ_{289}	−50.343	−1.167	−1.147
ϕ_{114}	16.303	0.068	0.075	ϕ_{299}	51.796	−1.269	−1.411
ϕ_{122}	160.087	−1.769	−2.377	ϕ_{333}	−214.052	−0.410	−0.428
ϕ_{123}	−38.258	0.107	0.182	ϕ_{334}	−60.291	0.174	−0.160
ϕ_{124}	1.057	−0.199	−0.282	ϕ_{344}	−10.553	0.992	0.295
ϕ_{133}	−11.563	−0.387	−0.361	ϕ_{355}	−118.613	0.029	0.065
ϕ_{134}	1.405	−0.056	0.000	ϕ_{366}	43.322	0.370	0.415
ϕ_{144}	2.496	−0.082	−0.032	ϕ_{367}	53.201	0.002	0.030
ϕ_{155}	279.227	−0.270	−0.196	ϕ_{377}	−62.228	−0.485	−0.072
ϕ_{166}	−1415.249	−22.728	−23.068	ϕ_{388}	−88.801	0.018	0.200
ϕ_{167}	4.793	0.207	0.196	ϕ_{389}	20.413	0.335	0.402
ϕ_{177}	303.156	−0.232	−0.127	ϕ_{399}	−316.983	0.832	0.839
ϕ_{188}	261.965	−1.344	−1.154	ϕ_{444}	−73.665	2.840	2.980
ϕ_{189}	−72.987	−0.408	−0.395	ϕ_{455}	48.524	−0.157	−0.139
ϕ_{199}	15.020	−0.199	−0.169	ϕ_{466}	20.879	0.173	0.179
ϕ_{222}	127.601	−28.071	−43.486	ϕ_{467}	6.462	−0.118	−0.096
ϕ_{223}	−25.107	0.939	0.578	ϕ_{477}	−24.364	−1.204	−0.701
ϕ_{224}	−21.061	1.654	2.547	ϕ_{488}	8.745	−0.741	−0.568
ϕ_{233}	19.224	−0.548	−0.392	ϕ_{489}	39.978	−0.332	−0.299
ϕ_{234}	3.908	−0.904	0.000	ϕ_{499}	−40.364	0.392	0.510
ϕ_{244}	13.605	−3.070	−3.397	ϕ_{568}	−277.347	−0.441	−0.389
ϕ_{255}	−68.021	−0.850	−0.655	ϕ_{569}	68.569	−0.208	−0.180
ϕ_{266}	−122.923	0.565	0.722	ϕ_{578}	−66.866	−1.052	−0.619
ϕ_{267}	−286.834	−0.598	−0.587	ϕ_{579}	−81.813	−0.657	−0.484

TABLE IV. The diagonal MP2 quartic force field of CH_2F_2 (cm^{-1}) in reduced normal coordinates.

ϕ_{1111}	511.953
ϕ_{2211}	− 190.170
ϕ_{2222}	35.238
ϕ_{3311}	− 2.690
ϕ_{3322}	− 4.207
ϕ_{3333}	25.646
ϕ_{4411}	0.999
ϕ_{4422}	− 1.893
ϕ_{4433}	− 2.893
ϕ_{4444}	16.715
ϕ_{5511}	− 236.450
ϕ_{5522}	− 0.651
ϕ_{5533}	7.890
ϕ_{5544}	− 4.729
ϕ_{5555}	97.253
ϕ_{6611}	547.047
ϕ_{6622}	− 252.869
ϕ_{6633}	− 5.315
ϕ_{6644}	2.597
ϕ_{6655}	− 238.659
ϕ_{6666}	572.728
ϕ_{7711}	− 227.288
ϕ_{7722}	70.476
ϕ_{7733}	− 3.426
ϕ_{7744}	− 3.149
ϕ_{7755}	48.414
ϕ_{7766}	− 233.428
ϕ_{7777}	110.941
ϕ_{8811}	− 234.639
ϕ_{8822}	13.363
ϕ_{8833}	9.610
ϕ_{8844}	− 4.886
ϕ_{8855}	80.324
ϕ_{8866}	− 254.636
ϕ_{8877}	30.513
ϕ_{8888}	63.372
ϕ_{9911}	− 4.255
ϕ_{9922}	5.010
ϕ_{9933}	79.280
ϕ_{9944}	− 16.029
ϕ_{9955}	− 2.652
ϕ_{9966}	− 5.449
ϕ_{9977}	4.556
ϕ_{9988}	4.879
ϕ_{9999}	85.447

TABLE V. The MP2 anharmonic (a) x_{rs} and (b) Darling–Dennison constants K_{rrss} (cm^{-1}) for CH_2F_2.

rs	(a)	(b)
11	− 28.517	
12	− 30.449	− 64.079
13	− 0.089	− 0.843
14	1.108	− 0.008
15	− 11.698	− 104.275
16	− 117.312	− 124.032
17	− 6.245	− 115.984
18	− 30.343	− 97.363
19	3.427	− 3.867
22	− 0.208	
23	− 3.826	− 0.620
24	− 1.611	− 0.570
25	− 2.998	− 23.768
26	− 19.011	− 120.578
27	− 16.559	− 15.254
28	− 1.191	− 56.378
29	− 3.113	− 0.688
33	− 3.570	
34	− 3.814	− 1.361
35	− 3.539	− 1.286
36	0.704	− 1.805
37	− 4.641	− 2.668
38	− 2.335	1.578
39	− 12.181	− 21.727
44	− 0.079	
45	0.128	− 2.776
46	2.025	− 0.228
47	− 1.568	− 1.878
48	− 1.603	− 1.965
49	− 6.447	− 3.301
55	− 4.216	
56	− 7.429	− 117.094
57	2.215	− 10.757
58	− 18.190	− 20.987
59	− 10.094	− 3.135
66	− 33.227	
67	− 3.420	− 120.461
68	− 12.178	− 117.967
69	5.482	− 5.467
77	− 1.974	
78	− 0.016	− 18.035
79	− 4.029	− 1.687
88	− 0.016	
89	− 7.902	− 1.536
99	− 4.481	

$$\begin{array}{c} \\ 3\omega_1 \\ 2\omega_1+\omega_6 \\ \omega_1+2\omega_6 \\ 3\omega_6 \end{array} \begin{pmatrix} 8770.76 & 0.00 & -107.42 & 0.00 \\ 0.00 & 8750.04 & 0.00 & -107.42 \\ -107.42 & 0.00 & 8840.46 & 0.00 \\ 0.00 & -107.42 & 0.00 & 9042.01 \end{pmatrix}. \tag{24}$$

Local modes have been a subject of considerable interest in recent years,[52] since they provide a satisfactory model for these highly excited stretching overtones in molecules with equivalent C–H bonds.[30] To show their relationship with our description, we define local coordinates for the two C–H bonds

$$\delta r_1 = \frac{1}{\sqrt{2}}(q_1 + q_6),$$
$$\delta r_2 = \frac{1}{\sqrt{2}}(q_1 - q_6), \tag{25}$$

and the corresponding harmonic vibrational wave functions

$$\psi^{\pm}_{n,m}(\delta r_1, \delta r_2) = N_{n,m} H^{\pm}_{n,m}(\delta r_1, \delta r_2) \times \exp\left[-\frac{\alpha}{2}(\delta r_1^2 + \delta r_2^2)\right], \tag{26}$$

where n,m are the two C–H vibrational quantum numbers,

TABLE VI. (a) Computed and (b) experimental frequencies (cm^{-1}).

	(a)	(b)
ν_4	517	528.5[a]
$2\nu_4$	1034	(1057)[a]
ν_9	1059	1090.1[a]
ν_3	1087	1113.2[a]
ν_7	1178	1177.9[a]
ν_5	1264	1262.0[a]
ν_8	1446	1435.0[a]
ν_2	1517	1508.0[a]
$\nu_4+\nu_9$	1571	1619[a]
$\nu_3+\nu_4$	1601	1642[a]
$\nu_4+\nu_7$	1694	1706[a]
$\nu_4+\nu_5$	1781	1791[a]
$\nu_3+\nu_9$	2134	2190[b]
$\nu_3+\nu_7$	2261	2285.7[b]
$\nu_5+\nu_7$	2444	2437.6[b]
$\nu_8+\nu_9$	2495	2516[b]
$\nu_2+\nu_9$	2573	2542.9[b]
$\nu_2+\nu_7$	2679	2653.7[b]
$2\nu_8$	2847	2838[b]
$\nu_2+\nu_8$	2962	2948[c]
ν_1	2993	2948[c]
$\nu_4+\nu_8+\nu_9$	3014	
$2\nu_2$	3056	
ν_6	3080	3014.3[a]
$\nu_3+\nu_6$	4168	4130[b]
$\nu_6+\nu_7$	4255	4189[b]
$\nu_2+\nu_6$	4579	4503.4[b]
$2\nu_1$	5825	5797.8[b]
$\nu_1+\nu_6$	5870	
$2\nu_6$	6115	

[a] Reference 1.
[b] Reference 4.
[c] Reference 16.

$N_{n,m}$ is a normalizing factor, and $\alpha = 4\pi^2\mu_{CH}\omega_m$, μ_{CH} being the reduced mass and ω_m the C–H harmonic frequency. In C_{2v} symmetry, we define the bidimensional symmetrized Hermite polynomials[53]

$$H^{\pm}_{n,m}(\delta r_1,\delta r_2) = (-1)^{n+m}\exp[\alpha(\delta r_1^2+\delta r_2^2)] \times\left(\frac{\partial^{n+m}}{\partial^n\delta r_1\partial^m\delta r_2}\pm\frac{\partial^{n+m}}{\partial^m\delta r_1\partial^n\delta r_2}\right) \times\exp[-\alpha(\delta r_1^2+\delta r_2^2)]. \quad (27)$$

By expressing the differential operators in Eq. (27) in normal coordinates q_1, q_6 and neglecting all differences between C–H ω_m and the normal ω_1, ω_6 frequencies, we convert Eqs. (26) and (27) to the normal coordinate basis. For the third C–H overtone, we obtain

$$\psi^{+}_{3,0}(\delta r_1,\delta r_2) = \frac{1}{2}\psi_{3,0}(q_1,q_6) + \frac{\sqrt{3}}{2}\psi_{1,2}(q_1,q_6),$$

$$\psi^{-}_{3,0}(\delta r_1,\delta r_2) = \frac{\sqrt{3}}{2}\psi_{2,1}(q_1,q_6) + \frac{1}{2}\psi_{0,3}(q_1,q_6),$$

$$\psi^{+}_{2,1}(\delta r_1,\delta r_2) = \frac{\sqrt{3}}{2}\psi_{3,0}(q_1,q_6) - \frac{1}{2}\psi_{1,2}(q_1,q_6),$$

$$\psi^{-}_{2,1}(\delta r_1,\delta r_2) = \frac{1}{2}\psi_{2,1}(q_1,q_6) - \frac{\sqrt{3}}{2}\psi_{0,3}(q_1,q_6). \quad (28)$$

The overlap matrix elements between the eigenvectors of the effective vibrational Hamiltonian (24) and the local vibrational wave functions (28)

	$\psi^{+}_{3,0}$	$\psi^{-}_{3,0}$	$\psi^{+}_{2,1}$	$\psi^{-}_{2,1}$
$3\nu_1$	0.92	0.00	0.39	0.00
$2\nu_1+\nu_6$	0.00	0.98	0.00	0.20
$\nu_1+2\nu_6$	0.39	0.00	0.92	0.00
$3\nu_6$	0.00	0.20	0.00	0.98

(29)

demonstrates the highly local mode character of the C–H overtone modes, which increases with the C–H vibrational quanta.

Our predictions are summarized in Table VII where we compare the lowest computed C–H overtone frequencies of A_1 and B_2 symmetry to the experimental frequencies measured in the liquid phase.[10]

The maximum discrepancy from experiment is 230 cm^{-1}; as expected, the splitting between the A_1 and the B_2 components approaches zero for higher overtones.[10]

B. Rotational constants

The ground state rotational and centrifugal distortion constants are compared to experiment in Table VIII. They provide an additional test of the accuracy of the MP2 harmonic and cubic force fields.

For excited vibrational states, one has the additional difficulty of Coriolis coupling, requiring the simultaneous treatment of the rotational sublevels of all interacting states and the explicit inclusion of the off-diagonal blocks of matrix elements [Eq. (13)].

In our treatment, ν_3–ν_7, ν_7–ν_9, ν_3–ν_9, ν_5–ν_7, and ν_2–ν_8 fall within the limits established for resonant Coriolis interactions leading to the four state $\{\nu_3,\nu_5,\nu_7,\nu_9\}$ and to

TABLE VII. (a) Computed and (b) experimental (Ref. 10) C–H overtones frequencies (cm^{-1}).

	(a)	(b)
$3\nu_1$	8 693	8 579
$2\nu_1+\nu_6$	8 715	
$4\nu_1$	11 375	11 219
$3\nu_1+\nu_6$	11 380	
$5\nu_1$	13 929	13 698
$4\nu_1+\nu_6$	13 930	
$6\nu_1$	16 360	
$5\nu_1+\nu_6$	16 360	

TABLE VIII. Ground state rotational constants A_0, B_0, C_0 (MHz), quartic (KHz), and sextic (Hz) centrifugal distortion constants: (a) computed; (b) experimental values from Ref. 3.

	(a)	(b)
A_0	48 656	49 143
B_0	10 366	10 605
C_0	9 056	9 250
Δ_J	10.965	11.167
Δ_{JK}	− 62.695	− 62.729
Δ_K	632.888	627.079
δ_J	2.075	2.152
δ_K	26.976	28.163
Φ_J	0.017	0.015
Φ_K	26.495	26.528
Φ_{JK}	0.071	0.118
Φ_{KJ}	− 4.948	− 5.170
ϕ_J	0.007	0.007
ϕ_{JK}	0.040	0.029
ϕ_K	5.219	5.728

TABLE IX. Vibration–rotation interaction constants α_r^β (MHz). The effects of resonant Coriolis interactions are: (a) included by diagonalizing the appropriate effective vibrotational Hamiltonian matrix (13); (b) not included and all Coriolis interactions treated by second-order perturbation theory; (c) experimental values from Ref. 5.

	(a)	(b)	(c)
α_1^a	161.995	161.995	
α_2^a	208.277	208.277	192.643
α_3^a	− 38.379	602.390	855.740
α_4^a	− 336.081	− 336.081	− 337.739
α_5^a	284.744	284.744	226.197
α_6^a	96.643	96.643	
α_7^a	132.486	− 508.243	− 750.714
α_8^a	187.783	187.783	119.545
α_9^a	427.635	427.635	444.03
α_1^b	− 7.841	− 7.841	
α_2^b	0.082	0.082	− 3.207
α_3^b	57.577	57.577	55.165
α_4^b	15.710	15.710	21.868
α_5^b	1.544	1.544	0.65
α_6^b	− 14.682	− 14.682	
α_7^b	27.644	− 1.354	− 8.155
α_8^b	1.046	1.046	− 3.635
α_9^b	46.644	75.662	73.610
α_1^c	− 8.298	− 8.298	
α_2^c	9.654	− 92.893	− 94.801
α_3^c	45.658	− 162.987	− 178.534
α_4^c	28.172	28.172	33.244
α_5^c	− 1.678	− 64.612	− 82.604
α_6^c	− 10.487	− 10.487	
α_7^c	18.464	81.398	96.715
α_8^c	10.989	113.536	114.288
α_9^c	48.547	257.192	269.311

the two state $\{\nu_2,\nu_8\}$ effective rotational Hamiltonians, whose structure is sketched in Fig. 1. Experimentally, the rotational analysis has been performed separately for each vibrational band.[4] This amounts to treating all Coriolis interactions (including resonant interactions) by perturbation theory [see the second term in Eq. (12)] neglecting resonant effects. To make possible the comparison with experiment, the vibration–rotation interaction constants α_r^β have been evaluated with and without the inclusion of resonant effects. The two set of values are compared to experiment in Table IX. The constants with the largest Coriolis contributions exhibit the major discrepancies from the experimental values. Due to the approximate treatment of the resonant Coriolis interactions in the analysis of experimental data, on the whole we consider, the comparison satisfactory.

In Table X, we compare to experiment the rotational constants evaluated for fundamentals, few overtones, and combination bands. A three state rotational analysis of the

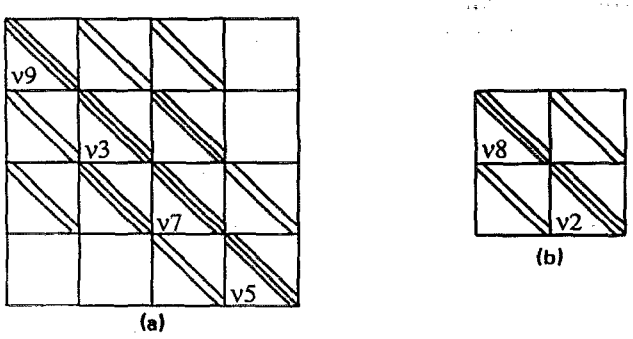

FIG. 1. The structure of the effective rotational Hamiltonian over the Wang basis (Ref. 58) for: (a) the ν_3, ν_7, ν_9, and ν_5 and (b) the ν_2, and ν_8 vibrotational states with explicit inclusion of Coriolis resonance interactions. The matrix elements in the off-diagonal blocks of the Hamiltonian matrix are given by Eq. (13) with the $\xi_{vv'}^\beta$ constants of Table XI [column (a)].

ν_3,ν_7,ν_9 bands is available,[9] making possible a more direct comparison of the two treatments of the Coriolis coupling for these fundamentals. By comparing the two sets of theoretical values, the effect of the ν_3–ν_7, ν_3–ν_9 Coriolis interactions on effective rotational constants is clearly seen. The A constants of ν_3 and ν_7 and the C constants of ν_3 and ν_9 are modified approximately by the same amount on opposite directions by 700 and 200 MHz, respectively; by comparison, the ν_7–ν_9 interaction is less important. The shift of the rotational constants from the ground state values is well reproduced in most cases.

To compare to experiment the off-diagonal Coriolis matrix elements,[13] we list in Table XI the computed values of the $\xi_{vv'}^\beta$ constants with the available experimental information.

C. Infrared intensities

The MP2 dipole analytic first derivatives μ_r^α with respect to reduced normal coordinates are listed in Table XII. Their absolute values are related to the infrared intensities to be discussed below; their relative signs have been determined experimentally from the analysis of Coriolis perturbations on intensities. Given the phases of the normal coordinates implied by the matrix elements in Table XI, the signs of μ_3^b,

TABLE X. Shifts (MHz) of rotational constants ΔA, ΔB, and ΔC from ground state values evaluated by Eq. (11) with the α_r^β constants of Table IX and comparison with the experimental values ΔA^{sper}, ΔB^{sper}, and ΔC^{sper}: (i) all Coriolis interactions treated by perturbation theory; (ii) variational treatment of resonant $\nu_3-\nu_7$, $\nu_3-\nu_9$, $\nu_7-\nu_9$, $\nu_5-\nu_7$, and $\nu_2-\nu_8$ Coriolis interactions. The first set of values is compared to the experimental values of Ref. 4 and the second to the experimental values of Ref. 9.

		ΔA	ΔB	ΔC	ΔA^{sper}	ΔB^{sper}	ΔC^{sper}
ν_1	(i)	−266.19	−51.14	−222.02			
ν_2	(i)	−208.28	−0.08	92.89	−192.64	3.21	93.83
ν_3	(i)	−599.29	−57.51	162.45	−855.74	−55.17	177.54
	(ii)	39.92	−57.51	−45.68	42.63	−59.34	−26.06
ν_4	(i)	336.08	−15.71	−28.17	337.8	−21.87	−33.21
ν_5	(i)	−284.74	−1.54	64.61	−266.20	−0.65	81.60
ν_6	(i)	−96.64	14.68	10.49			
ν_7	(i)	508.28	1.35	−81.40	750.71	8.16	−97.71
	(ii)	−132.49	−27.66	−18.46	−140.90	−20.29	−97.65
ν_8	(i)	−186.55	−2.21	−115.74	−119.55	3.64	−115.29
ν_9	(i)	−427.63	−75.66	−257.19	−444.03	−73.59	−270.29
	(ii)	−427.63	−46.64	−48.55	−436.53	−65.78	−65.79
$2\nu_4$	(i)	669.06	−31.48	−55.81	672.86	−43.77	−68.27
$\nu_3+\nu_4$	(i)	−255.84	−73.07	133.01	−496.92	−74.02	116.96
$\nu_5+\nu_4$	(i)	51.34	−17.25	36.44	66.84	−23.26	42.92
$\nu_4+\nu_7$	(i)	844.36	−14.36	−109.57	1089.01	−15.12	−126.68
$\nu_9+\nu_4$	(i)	−92.79	−90.21	−283.16	−102.37	−94.87	−267.76
$3\nu_4$	(i)	997.77	−47.34	−82.71	1004.01	−65.51	−107.05

μ_7^c, and μ_9^a have been determined[16] $-,+,-$ or $+,-,+$ in agreement with the computed signs. Moreover, we predict identical signs of μ_2^b and μ_8^a as found in CD_2F_2, where ν_2 and ν_8 are strongly coupled by Coriolis interaction.[16]

Dipole second and third derivatives evaluated by the mixed analytic-numerical procedure described in Sec. II C are listed in Tables XIII and XIV, respectively.

From Tables XII–XIV, we evaluate the harmonic [Eq. (15a)] and the anharmonic [Eqs. (15b)–(15g)] components of the vibrational transition moments. The detailed list of all contributions is given for fundamentals in Table XV. The corresponding harmonic and total anharmonic intensities are given for fundamentals, selected overtones, and combination bands in Table XVI [columns (a) and (b)]. We finally include the contributions of the resonant Fermi and Darling–Dennison interactions using the eigenvectors of the corresponding effective vibrational Hamiltonians as described in Sec. IV A [column (c) in Table XVI].

As shown in Table XV, all nonresonant anharmonic contributions to the vibrational transition moments were found small for all fundamentals.

Anharmonic corrections to the infrared intensities are essential for overtones and combination bands whose intensities vanish in the harmonic approximation. The polarization of all vibrational bands listed in Table XVI agree with the experimental assignments.[1] An additional anharmonic contribution to the infrared intensities, originating from Watson's correction to the vibrational kinetic energy operator,[54] has been estimated[37,55] to be negligible in all cases.

The harmonic intensity of the ν_1 band has been computed as 38.36 km mol^{-1} to be compared with a previous theoretical estimate of 46.21 km mol^{-1} (Ref. 24) and with the experimental values of 22.4, 29.8, and 23.6 km mol^{-1}.[12,13,16] By perturbation theory, we have estimated the overall anharmonic contribution to the intensity of this band −1.69 km mol^{-1} and so this is not the major cause of the discrepancy in the intensity of this band. The complex pattern of Fermi and Darling–Dennison interactions leading to the ef-

TABLE XI. ξ_{uv}^β constants for the off-diagonal blocks of the effective rotational Hamiltonian [see Eq. (13)]: (a) computed values; (b) experimental values from Ref. 9.

	(a)	(b)
$\xi^c_{\nu_8\nu_2}$	0.494 7	
$\xi^c_{\nu_9\nu_3}$	0.409 8	0.3796
$\xi^a_{\nu_7\nu_3}$	1.372 82	1.411
$\xi^b_{\nu_9\nu_7}$	−0.329 65	−0.4704
$\xi^c_{\nu_7\nu_5}$	0.451 76	

TABLE XII. The MP2 dipole moment first derivatives μ_r^α (10^{-2} D).

μ_r^α	
μ_1^b	9.883
μ_2^b	1.588
μ_3^b	−26.491
μ_4^b	8.462
μ_6^c	−7.957
μ_7^c	10.698
μ_8^a	8.588
μ_9^a	−43.158

TABLE XIII. The MP2 dipole moment second derivatives μ^{α}_{rs} (10^{-2} D).

μ^{α}_{rs}		μ^{α}_{rs}	
μ^{b}_{11}	1.425	μ^{a}_{38}	−0.312
μ^{b}_{12}	0.544	μ^{a}_{39}	1.174
μ^{b}_{13}	−1.592	μ^{b}_{44}	−0.567
μ^{b}_{14}	−0.378	μ^{c}_{46}	0.278
μ^{c}_{16}	−2.359	μ^{c}_{47}	−0.061
μ^{c}_{17}	0.863	μ^{a}_{48}	0.367
μ^{a}_{18}	−1.032	μ^{a}_{49}	−0.945
μ^{a}_{19}	−0.281	μ^{b}_{55}	3.049
μ^{b}_{22}	1.960	μ^{a}_{56}	0.631
μ^{b}_{23}	−0.190	μ^{a}_{57}	−0.308
μ^{b}_{24}	−0.311	μ^{c}_{58}	1.685
μ^{c}_{26}	−2.782	μ^{c}_{59}	0.247
μ^{c}_{27}	−2.271	μ^{b}_{66}	2.644
μ^{a}_{28}	0.917	μ^{b}_{67}	−1.154
μ^{a}_{29}	0.732	μ^{b}_{77}	0.696
μ^{b}_{33}	0.667	μ^{b}_{88}	2.635
μ^{b}_{34}	0.555	μ^{b}_{89}	0.576
μ^{c}_{36}	1.984	μ^{b}_{99}	0.511
μ^{c}_{37}	−0.606		

TABLE XIV. The MP2 dipole moment third derivatives μ^{α}_{rst} (10^{-2} D).

μ^{α}_{rst}		μ^{α}_{rst}	
μ^{b}_{111}	−0.132	μ^{b}_{344}	0.081
μ^{b}_{112}	0.001	μ^{b}_{355}	−0.372
μ^{b}_{113}	−0.077	μ^{b}_{366}	−0.192
μ^{b}_{114}	−0.016	μ^{b}_{377}	−0.038
μ^{c}_{116}	−0.085	μ^{b}_{388}	−0.191
μ^{c}_{117}	0.167	μ^{b}_{399}	−0.114
μ^{a}_{118}	0.270	μ^{b}_{444}	0.001
μ^{a}_{119}	0.016	μ^{c}_{446}	0.078
μ^{b}_{122}	0.176	μ^{c}_{447}	−0.044
μ^{b}_{133}	0.107	μ^{a}_{448}	−0.046
μ^{b}_{144}	−0.103	μ^{a}_{449}	0.111
μ^{b}_{155}	−0.072	μ^{b}_{455}	−0.048
μ^{b}_{166}	−0.013	μ^{b}_{466}	−0.068
μ^{b}_{177}	−0.143	μ^{b}_{477}	−0.023
μ^{b}_{188}	−0.153	μ^{b}_{488}	−0.051
μ^{b}_{199}	0.178	μ^{b}_{499}	−0.012
μ^{b}_{222}	−0.658	μ^{c}_{556}	−0.196
μ^{b}_{223}	−0.206	μ^{c}_{557}	0.136
μ^{b}_{224}	−0.100	μ^{a}_{558}	−0.830
μ^{c}_{226}	0.097	μ^{a}_{559}	−0.035
μ^{c}_{227}	−0.956	μ^{c}_{666}	0.261
μ^{a}_{228}	−0.412	μ^{c}_{667}	0.590
μ^{a}_{229}	−0.016	μ^{a}_{668}	0.408
μ^{b}_{233}	0.145	μ^{a}_{669}	0.022
μ^{b}_{244}	−0.005	μ^{c}_{677}	−0.041
μ^{b}_{255}	0.047	μ^{c}_{688}	−0.215
μ^{b}_{266}	0.661	μ^{c}_{699}	−0.237
μ^{b}_{277}	−0.510	μ^{c}_{777}	0.019
μ^{b}_{288}	−0.320	μ^{a}_{778}	−0.380
μ^{b}_{299}	0.160	μ^{a}_{779}	0.069
μ^{b}_{333}	0.024	μ^{c}_{788}	0.031
μ^{b}_{334}	−0.137	μ^{c}_{799}	0.075
μ^{c}_{336}	−0.235	μ^{a}_{888}	−1.160
μ^{c}_{337}	0.055	μ^{a}_{889}	0.083
μ^{a}_{338}	0.092	μ^{a}_{899}	0.283
μ^{a}_{339}	0.002	μ^{a}_{999}	−0.717

TABLE XV. Harmonic [Eq. (15a)] and anharmonic contributions [Eqs. (15d)–(15g)] to the vibrational transition moments for fundamentals evaluated by perturbation theory (10^{-2} D).

ν_r	α	(15a)	(15d)	(15e)	(15f)	(15g)	Total
ν_1	(a)	0	0	0	0	0	0
	(b)	6.988	−0.027	0.643	0.004	−0.602	7.006
	(c)	0	0	0	0.025	0	0.025
ν_2	(a)	0	0	0	−0.004	0	−0.004
	(b)	1.123	−0.085	0.053	−0.399	0.024	0.716
	(c)	0	0	0	0.021	0	0.021
ν_3	(a)	0	0	0	−0.028	0	−0.028
	(b)	−18.732	−0.192	0.031	−0.101	−0.027	−19.020
	(c)	0	0	0	−0.036	0	−0.036
ν_4	(a)	0	0	0	0	0	0
	(b)	5.984	−0.080	−0.013	0.064	−0.072	5.883
	(c)	0	0	0	0.011	0	0.011
ν_5	(a)	0	0	0	−0.001	0	−0.001
	(b)	0	0	0	0.130	0	0.130
	(c)	0	0	0	−0.029	0	−0.029
ν_6	(a)	0	0	0	−0.001	0	−0.001
	(b)	0	0	0	0.026	0	0.026
	(c)	−5.627	−0.101	−0.711	−0.053	0	−6.224
ν_7	(a)	0	0	0	0.051	0	0.051
	(b)	0	0	0	−0.095	0	−0.095
	(c)	7.565	0.013	0.003	0.051	0	7.690
ν_8	(a)	6.072	−0.314	−0.047	−0.399	0.206	5.519
	(b)	0	0	0	0.001	0	0.001
	(c)	0	0	0	0.015	0	0.015
ν_9	(a)	−30.517	−0.082	0.132	−0.140	−0.101	−30.708
	(b)	0	0	0	0.016	0	0.016
	(c)	0	0	0	0.020	0	0.020

fective vibrational Hamiltonian (23) splits the overall ν_1 intensity into four vibrational bands, the one at lowest frequency being $2\nu_8$ (see Table VI). This band is well isolated in the infrared spectrum. Its intensity has been measured directly as 6.8 ± 0.6 km mol^{-1} which compares well with our value of 4.05 km mol^{-1}. The b polarization of the band[16] is also consistent with the computed polarization. The higher frequency bands ν_1, and $\nu_4 + \nu_8 + \nu_9$ are nearly degenerate (see Table VI) with equal intensities and polarizations (Table XVI), thus explaining the presence of two degenerate b bands in the infrared spectrum at 2948 cm^{-1}[16] with a total computed intensity of 20.4 km mol^{-1}. The assignment of the extra band to $\nu_2 + \nu_8$[16] is not supported by our results due to the low intensity and the a polarization computed for this band; a very strong resonant enhancement of its intensity through $2\nu_2$ and $\nu_2 + \nu_8$ Coriolis interaction is also unlikely given the frequency gap separating these two bands (see Table VI). Finally, the high intensity of $2\nu_2$ originates from Fermi interaction with ν_1 and from the Darling–Dennison interaction with $2\nu_8$, suggesting an assignment of the ν_1 and ν_6 bands to the $\nu_1,\nu_4 + \nu_8 + \nu_9$ and to the $\nu_6,2\nu_2$ doublets, respectively, which bring the computed and the experimental frequency and intensity patterns in close agreement with experiment.

The ν_3, ν_7, ν_9, and ν_5 bands provide an interesting example of Coriolis interactions as shown by the effective rotational Hamiltonian of Fig. 1. The ν_3–ν_7 interaction, which originates from rotation about the a axis is the most important as seen by the coupling constants in Table XI and by the rotational constants in Table X. To show its effect on intensities, we consider a simplified description where only this interaction is explicitly taken into account. This amounts to converting the Hamiltonian of Fig. 1 into separate effective rotational Hamiltonians for ν_5 and ν_9 and for the ν_3,ν_7 pair of states. For the latter pair, we introduce the additional approximation of considering the molecule a symmetric top, which is justified by the computed (-0.935) and the experimental (-0.932) values of the asymmetry parameter κ and is expected to fail only for very low values of the rotational quantum number k. The effective rotational Hamiltonian is set easily in the symmetric top basis[56,57] to obtain approximate rotational wave functions for the pair of interacting states and the corresponding line intensities.[58] The resulting spectral profiles are shown separately for the ν_3 and ν_7 bands in Fig. 2. It is seen that the main effect of the interaction is to enhance the P-type subband of ν_7 and the R-type subband of ν_3. This corresponds to a positive Coriolis perturbation,[57] which agrees with the spectral profile of the ν_3,ν_7,ν_9 system of bands.[16] The intensity ratios computed for the three vibrational bands 0.687: 0.267: 0.047 are virtually coincident with those obtained from experiment.[16] The Coriolis effects on intensities can be deduced qualitatively from Fig. 2. The absolute intensities computed for the ν_9 band lies within the experimental values determinated from integrated intensities[12,13,16] and by sub-Doppler laser Stark spectroscopy.[17]

TABLE XVI. Infrared intensities (km mol^{-1}) and polarization of fundamentals, selected overtones, and combination bands: (a) harmonic approximation; (b) anharmonic corrections included by perturbation theory; (c) variational corrections for resonant Fermi and Darling–Dennison interactions included; (d) experimental (polarizations and) intensities.

Band	Polarization[a]	(a)	(b)	(c)	(d)	(d)
ν_4	*b*	4.69	4.49	4.49	4.80[b]	
$2\nu_4$	*b*	0	0.35	1.14		
ν_9	*a*	253.40	250.35		230.40[b]	316.49[c]
ν_3	*b*	97.55	98.58	97.76	89.50[b]	
ν_7	*c*	17.20	17.46		14.40[b]	
ν_5	*b*	0	0.01			
ν_8	*a*	13.72	11.05	10.51	10.30[b]	
ν_2	*b*	0.49	0.19			
$\nu_4 + \nu_9$	*a*	0	0.29	0.86		
$\nu_3 + \nu_4$	*b*	0	0.33	0.32		
$\nu_4 + \nu_7$	*c*	0	0.01			
$\nu_4 + \nu_5$		0	0			
$\nu_3 + \nu_9$	*a*	0	3.84	3.83		
$\nu_3 + \nu_7$	*a*	0	0.17	0.17		
$\nu_5 + \nu_7$	*a*	0	0.11			
$\nu_8 + \nu_9$	*b*	0	0.21	0.21		
$\nu_2 + \nu_9$	*a*	0	0.01			
$\nu_2 + \nu_7$	*c*	0	0.01			
$2\nu_8$	*b*	0	0.70	4.05	6.8[b]	
$\nu_2 + \nu_8$	*a*	0	0.30	0.29		22.4[b]
ν_1	*b*	38.36	36.67	10.39	15.6[b]	
$\nu_4 + \nu_8 + \nu_9$	*b*	0	0	9.99		
$2\nu_2$	*b*	0	0.36	13.61		
ν_6	*c*	25.57	29.91		42.20[b]	
$\nu_3 + \nu_6$	*c*	0	0.86	0.85		
$\nu_6 + \nu_7$	*c*	0	0.29			
$\nu_2 + \nu_6$	*c*	0	1.59			
$2\nu_1$		0	0	0		
$\nu_1 + \nu_6$	*c*	0	0.49	0.25		
$2\nu_6$	*b*	0	0.26	0.21		

[a] Reference 1.
[b] Reference 16.
[c] Reference 17.

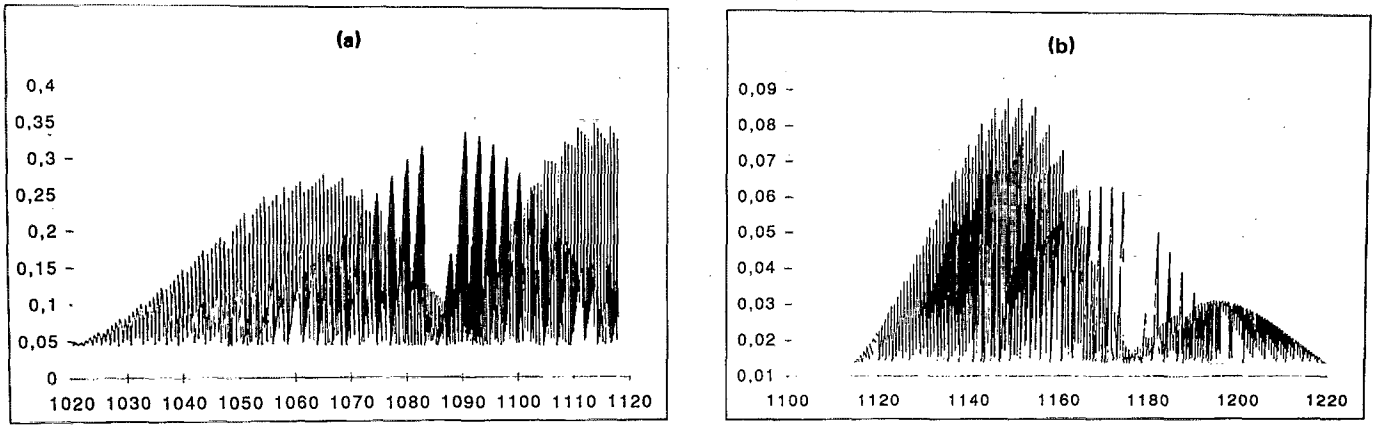

FIG. 2. Computed spectral profiles of (a) ν_3 and (b) ν_7 bands using symmetric top rotational wave functions and theoretical values of vibrational frequencies, rotational, and Coriolis coupling constants (see the text). Theoretical frequencies and relative intensities on the x and y axes, respectively.

CONCLUSIONS

The harmonic and the anharmonic components of the molecular force and dipole fields have been evaluated with the inclusion of electron correlation effects as accounted for by the MP2 method using a large basis set. From these, the anharmonic vibrational frequencies, rotational constants, and intensities have been evaluated for all fundamentals, selected overtones, and combination bands. All nonresonant anharmonic contributions to the vibrational transition moments were found small for all fundamentals. Only for the ν_1 band intensity, we predict large anharmonic corrections due to nearly resonant Fermi and Darling–Dennison interactions. The large quantity of spectroscopic data available for this molecule has allowed a detailed comparison of the theoretical values with the experiment and a satisfactory description of all vibration and vibration–rotation molecular properties has been achieved. From the results of this study, we conclude that the present type of theoretical treatment is able to provide accurate information on most spectroscopic properties and may be useful to supplement low and high resolution spectral data and build reliable models for their analysis.

ACKNOWLEDGMENTS

This work was completed while P. P. was visiting the Theoretical Chemistry Department of Cambridge and he wishes to acknowledge the kind hospitality at the department. Financial support from CNR (Italy) within Progetto Finalizzato Sistemi Informatici e Calcolo Parallelo is also acknowledged.

[1] I. Suzuki and T. Shimanouchi, J. Mol. Spectrosc. **46**, 130 (1973).
[2] J. A. Koutcher, R. H. Larkin, J. R. Williams, and S. G. Kukolich, J. Mol. Spectrosc. **60**, 373 (1976).
[3] L. Martinache, D. Boucher, J. Demaison, and J. C. Deroche, J. Mol. Spectrosc. **119**, 225 (1986).
[4] E. Hirota, J. Mol. Spectrosc. **69**, 409 (1978).
[5] E. Hirota, J. Mol. Spectrosc. **71**, 145 (1978).
[6] M. Carlotti, D. G. Nivellini, F. Tullini, and B. Carli, J. Mol. Spectrosc. **132**, 158 (1988).
[7] T. A. De Temple and E. J. Danielewicz, in *Infrared and Millimeter Waves*, edited by K. J. Button (Academic, New York, 1983), Vol. 7.
[8] E. J. Danielewicz, F. Galantowicz, F. B. Foote, R. D. Reel, and D. T. Hodges, Opt. Lett. **4**, 280 (1979).
[9] E. L. Khadir Benichou, thesis, Université de Paris Sud, 1984.
[10] B. R. Henry and I. Fu Hung, Chem. Phys. **29**, 465 (1978).
[11] R. Wallace and A. A. Wu, Chem. Phys. **39**, 221 (1979).
[12] J. Morcillo, L. J. Zamorano, and J. M. V. Hereda, Spectrochim. Acta **22**, 1969 (1966).
[13] M. Mizuno and S. Saeki, Spectrochim. Acta Part A **32**, 1077 (1976).
[14] J. H. Newton, R. A. Levine, and W. B. Person, J. Chem. Phys. **67**, 3282 (1977).
[15] T. A. Ford, R. Aroca M., and E. A. Robinson, Spectrochim. Acta Part A **34**, 77 (1978).
[16] S. Kondo, T. Nakanaga, and S. Saeki, J. Chem. Phys. **73**, 5409 (1980).
[17] B. Zhang, Xijia Gu, N. R. Isenor, and G. Scodes, Chem. Phys. **126**, 151 (1988).
[18] C. E. Blom and A. Muller, J. Mol. Spectrosc. **70**, 449 (1978).
[19] J. F. Gaw. N. C. Handy, P. Palmieri, and A. Degli Esposti, J. Chem. Phys. **89**, 959 (1988).
[20] N. C. Handy, NATO ASI Ser. **277**, 23 (1989).
[21] A. Willets, J. F. Gaw, N. C. Handy, and S. Carter, J. Mol. Spectrosc. **135**, 370 (1989).
[22] E. D. Simandiras, J. E. Rice, T. J. Lee, R. D. Amos, and N. C. Handy, J. Chem. Phys. **88**, 3187 (1988).
[23] N. C. Handy, R. D. Amos, J. F. Gaw, J. E. Rice, and E. D. Simandiras, Chem. Phys. Lett. **120**, 151, (1985).
[24] G. L. Fox and H. B. Schlegel, J. Chem. Phys. **92**, 4351, (1990).
[25] R. D. Amos and J. E. Rice, the Cambridge analytic derivatives package, (CADPAC), Cambridge, Mass., 1987.
[26] R. J. Whitehead and N. C. Handy, J. Mol. Spectrosc. **59**, 459 (1976).
[27] H. Romanowski, J. M. Bowman, and L. B. Harding, J. Chem. Phys. **82**, 4155 (1985).
[28] A. Nauts and R. E. Wyatt, Phys. Rev. A **30**, 872 (1984).
[29] K. M. Dunn, J. E. Boggs, and P. Pulay, J. Chem. Phys. **86**, 5088 (1987).
[30] I. M. Mills and A. G. Robiette, Mol. Phys. **56**, 743 (1985).
[31] G. Herzberg, *Infrared and Raman Spectra* (Van Nostrand–Reinhold, New York, 1945).
[32] I. M. Mills, in *Molecular Spectroscopy: Modern Research*, edited by K. Narahari Rao and C. W. Mathews (Academic, New York, 1972), pp. 115–140.
[33] I. M. Mills, *Theoretical Chemistry, Specialist Periodical Report* (The Chemical Society, London, 1974), Vol. 1, pp. 100–159.
[34] J. K. Watson, in *Vibrational Spectra and Structure*, edited by J. R. Durig (Elsevier, New York, 1977), Vol. 6, pp. 1–89.
[35] D. Papousek and M. R. Aliev, *Molecular Vibrational Spectra* (Elsevier, New York, 1982).
[36] S. Califano, *Vibrational States* (Wiley, London, 1976).
[37] J. F. Gaw, A. Willetts, W. H. Green, Jr., and N. C. Handy, in *Advances in Molecular Vibrations and Collision Dynamics*, edited by J. M. Bowman (JAI, Greenwich, CT, 1991).
[38] A. Willetts, N. C. Handy, W. H. Green, and D. Jayatilaka, J. Phys. Chem. **94**, 5608 (1990).
[39] E. Fermi, Z. Phys. **71**, 251 (1931).
[40] B. T. Darling and D. M. Dennison, Phys. Rev. **57**, 128 (1940).
[41] W. J. Hehre, R. Ditchfield, and J. A. Pople, J. Chem. Phys. **54**, 724 (1971).
[42] The 631G-extended basis is produced by adding extra functions to the 631G (Ref. 41) basis. In the present case, the extra functions are: for hydrogen *s*—0.054 and *p*—0.75 and 0.25; for carbon *s*—0.056, *p*—0.056, and *d*—0.8 and 0.266; for fluorine, *s*—0.119, *p*—0.119, and *d*—1.5 and 0.5.
[43] W. Schneider and W. Thiel, Chem. Phys. Lett. **157**, 367 (1989).
[44] J. L. Duncan, D. C. McKean, and G. K. Speirs, Mol. Phys. **24**, 553 (1972).
[45] A. R. Hoy, I. M. Mills, and G. Strey, Mol. Phys. **24**, 1265 (1972).
[46] The set of curvilinear coordinates is defined in Ref. 19. We have kept the order within each symmetry block and rearranged the blocks in the order A_1, A_2, B_1, B_2.
[47] J. L. Duncan, G. D. Nivellini, and F. Tullini, J. Mol. Spectrosc. **118**, 145 (1986).
[48] S. Kondo and Y. Koga, J. Chem. Phys. **69**, 4022 (1978).
[49] H. B. Stewart and H. H. Nielsen, Phys. Rev. **75**, 640 (1949); D. H. Rank, E. R. Shull, and E. L. Pace, J. Chem. Phys. **18**, 885, (1950); W. Holzer, J. Mol. Spectrosc. **26**, 123 (1968).
[50] S. Reichman and J. Overend, J. Chem. Phys. **47**, 1525 (1967).
[51] G. Herzberg, *Infrared and Raman Spectra of Polyatomic Molecules* (Van Nostrand, New York, 1945).
[52] M. S. Child and L. Halonen, Adv. Chem. Phys. **57**, 1 (1984).
[53] H. Eyring, J. Walter, and G. E. Kimball, *Quantum Chemistry* (Wiley, New York, 1964), p. 61.
[54] J. K. G. Watson, Mol. Phys. **15**, 470 (1968).
[55] G. Amat, H. H. Nielsen, and G. Tarrago, *Rotation–Vibration of Polyatomic Molecules* (Marcel Dekker, New York, 1971).
[56] I. M. Mills, Pure Appl. Chem. **11**, 325 (1965).
[57] J. M. Hollas, *High Resolution Spectroscopy* (Butterworths, London, 1982), p. 227.
[58] S. C. Wang, Phys. Rev. **34**, 243 (1929).